Bulletin of the New Zealand Society for Earthquake Engineering, Vol. XX, No. Y, Month 2016

SEISMIC EARTH FORCES AGAINST EMBEDDED RETAINING WALLS: INSIGHTS FROM NUMERICAL MODELLING

C.Y. Chin[1], Claudia Kayser[2] and Michael Pender[3]

(Submitted *December 2015*; Reviewed *February 2016*; Accepted *March 2016*)

ABSTRACT

This paper provides results from carrying out two-dimensional dynamic finite element analyses to determine the applicability of simple pseudo-static analyses for assessing seismic earth forces acting on embedded cantilever and propped retaining walls appropriate for New Zealand. In particular, this study seeks to determine if the free-field Peak Ground Acceleration (PGA_{ff}) commonly used in these pseudo-static analyses can be optimized. The dynamic finite element analyses considered embedded cantilever and propped walls in shallow (Class C) and deep (Class D) soils (NZS 1170.5:2004). Three geographical zones in New Zealand were considered. A total of 946 finite element runs confirmed that optimized seismic coefficients based on fractions of PGA_{ff} can be used in pseudo-static analyses to provide moderately conservative estimates of seismic earth forces acting on retaining walls. Seismic earth forces were found to be sensitive to and dependent on wall displacements, geographical zones and soil classes. A re-classification of wall displacement ranges associated with different geographical zones, soil classes and each of the three pseudo-static methods of calculations (Rigid, Stiff and Flexible wall pseudo-static solutions) is presented. The use of different ensembles of acceleration-time histories appropriate for the different geographic zones resulted in significantly different calculated seismic earth forces, confirming the importance of using geographic-specific motions. The recommended location of the total dynamic active force (comprising both static and dynamic forces) for all cases is 0.7H from the top of the wall (where H is the retained soil height).

INTRODUCTION

The determination of seismic earth pressures acting against retaining walls is a complex soil-structure interaction problem. Factors which affect these earth pressures include:

1. The nature of the input motions which includes the amplitude, frequency, directivity and duration of the motion.
2. The response of the soil behind, in front & underlying the wall.
3. The characteristics of the wall, which includes the strength and bending stiffness of the wall.

Due largely to its simplicity, the most common class of analysis for determining the magnitude and distribution of seismic earth pressure acting on a retaining wall is the pseudo-static analysis. This analysis makes use of the free-field Peak Ground Acceleration (PGA_{ff}) typically obtained from national design standards (e.g., NZ Transport Agency [1]). In addition, depending on expected wall displacements under gravity and seismic loading, there are three common solutions associated with this class of analysis. These three solutions are categorised according to increasing retaining wall displacements typically described as Rigid, Stiff or Flexible wall solutions. Since the early work of Okabe [2] and Mononobe & Matsuo [3] in establishing the Mononobe-Okabe (M-O) solution for flexible walls, numerous studies have been carried out to identify whether the full PGA_{ff} identified as the seismic coefficient employed in the M-O solution should be used, or whether a reduction (or increase) to PGA_{ff} can be applied. A similar question can also be asked for the Stiff and Rigid wall solutions which also incorporate the use of PGA_{ff}.

This study was undertaken in order to provide some evidence to support any reduction (or increase) to PGA_{ff} when used as a seismic coefficient in pseudo-static analysis, particularly for New Zealand. In addition, there would also be an opportunity to clarify what displacement ranges, in response to a seismic thrust, might be appropriate for the Rigid, Stiff and Flexible wall solutions. A non-linear dynamic finite element program, OpenSees (Open System for Earthquake Engineering Simulation), was used to carry out a number of analyses of embedded propped & cantilever retaining walls for shallow & deep soils subject to accelerations appropriate for three geographical areas in the North & South Island of New Zealand. From these analyses, seismic earth forces acting against retaining walls were determined and compared with pseudo-static solutions.

The three main objectives of this study were to:

1. Compare seismic soil thrusts from OpenSees finite element modelling against pseudo-static analytical methods such as the Rigid, Stiff and Flexible wall solutions & determine if a reduction (or increase) to PGA_{ff}, applied as a seismic coefficient to these solutions, can be justified.
2. Identify the range of wall displacements applicable to the pseudo-static solutions.
3. Determine the location of seismic active soil thrust acting on the retaining wall. This is frequently debated and important particularly for determining the magnitude of bending moment in the retaining wall.

[1] *Corresponding Author, Technical Director, Beca Ltd, Formerly Industry Fellow, UC Quake Centre, Christchurch, cy.chin@beca.com (Member)*
[2] *Geotechnical Engineer, AECOM, Formerly Industry Fellow, UC Quake Centre, Christchurch, ckay008@aucklanduni.ac.nz*
[3] *Professor, University of Auckland, Auckland, m.pender@auckland.ac.nz (Life Member)*

LITERATURE REVIEW

Pseudo-Static Analyses

Rigid Wall Response

Mathewson et al. [4] and Wood & Elms [5] both refer to the determination of the dynamic earth pressure for rigid walls as an incremental increase over static earth pressures calculated using the at-rest (K_o) earth pressure coefficient following the solution as proposed in Figure 1a. This simplified solution is based on elastic solutions developed by Wood [6]. Being a rigid wall response, no wall displacements are assumed.

Stiff Wall Response

Mathewson et al. [4] describes that for a relatively stiff wall, the earthquake pressures shown in Figure 1b could be assumed. They recommend that a movement at the top of the wall of between 0.1%H and 0.2%H under combined static and dynamic thrusts would be needed to obtain this reduction (i.e., 25% reduction) from the rigid wall pressure. This stiff wall earthquake pressure is an incremental increase over static earth pressures calculated using the active (K_A) earth pressure coefficient. This method of determining earthquake-induced pressures is also cited by Wood & Elms [5], although they recommend its use for top of wall movements of between 0%H to 0.2%H. This is a potential issue as 0%H is, in effect, a rigid wall response.

Flexible Wall Response

The flexible wall response typically uses the Mononobe-Okabe (M-O) solution [2, 3], which assumes that sufficient wall movement will need to occur to allow active conditions to develop and subsequently provides a convenient method of determining the total active thrust acting on retaining walls. Seed & Whitman [7] suggested that the total active thrust could be divided into two components comprising the initial static force (calculated using the active earth pressure coefficient, K_A) and a dynamic incremental force (calculated using ($K_{AE} - K_A$), refer to Figure 1c). Various publications differ on the magnitude of outward wall deformations (Δh) to allow the use of the M-O solution. These are expressed as ratios of Δh to the exposed wall height (H); $\Delta h / H$ expressed as a percentage. The range of $\Delta h / H$, which the M-O solution is said to apply, varies from $\Delta h / H > 0.1\%$ [8] to $\Delta h / H > 0.5\%$ [4, 5].

Notes:

- C_o is Peak Ground Acceleration coefficient referred to as PGA_{ff}/g in this study
- ΔP_{OE}, ΔP_E and ΔP_{AE} are referred to, as $\Delta P_{AE,Rigid\ Wall,100\%PGA}$, $\Delta P_{AE,Stiff\ Wall,100\%PGA}$ and $\Delta P_{AE,M-O,100\%PGA}$ respectively in this study with the subscript term $_{100\%PGA}$ referring to 100% of PGA_{ff}
- H is the retained soil height

Variations of Seismic Coefficients in Pseudo-Static Analyses

There have been many studies undertaken to establish the validity of the M-O solution. In particular, authors have had differing views on whether the use of PGA_{ff} as the seismic coefficient in the M-O solution results in unconservative, reasonable or conservative solutions. For this study, an unconservative solution would be one where the M-O solution under-predicts the actual dynamic pressure. In comparison, a conservative M-O solution over-predicts the actual dynamic pressure.

An example of a study where the use of PGA_{ff} results in smaller, unconservative values was reported by Green et al. [9]. Seed & Whitman [7] and Steedman & Zeng [10] reported reasonably matching values of M-O solutions using PGA_{ff}. More recently, reports by Gazetas et al. [11], Psarropoulos et al.[12], Anderson et al. [13] and Atik & Sitar [14] have suggested that use of PGA_{ff} in M-O solutions can be conservative. Anderson et al. [13] described the effects of wave-scattering and proposed height-dependent scaling factors to reduce $PGAs_{ff}$ to be used in M-O solutions for deriving earth pressures. They used US-centric acceleration motions and demonstrated differences in these scaling factors as a function also of location within the United States (Western, Central or Eastern US). Using centrifuge model testing and OpenSees numerical analysis of cantilever walls, Atik & Sitar [14] propose amongst other recommendations that for both stiff and flexible walls, using 65% of the PGA with the M-O method provides a good agreement with measured and calculated pressures. As the seismic events used by the above authors have unique seismic signatures which may not apply to New Zealand, the basis of this study was to carry out two-dimensional dynamic numerical analyses based on acceleration records which would be applicable to New Zealand.

PEAK GROUND ACCELERATIONS

Ground Motions Applicable to New Zealand

Various characteristics of seismic motions (including PGA, frequency content, directivity and duration) are known to influence the response of soil, and consequently the dynamic soil pressures acting against the retaining wall.

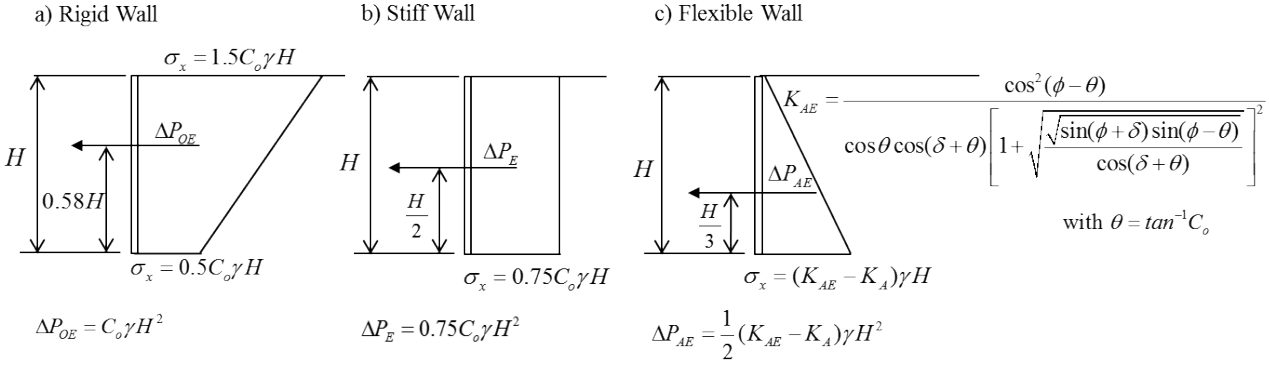

Figure 1: Earthquake induced pressures on a) Rigid wall [4], b) deformable (or Stiff) wall [4] and c) Flexible wall (from Seed & Whitman [7], based on Okabe [2] and Mononobe & Matsuo [3]).

For this study, soil classes were obtained from NZS 1170.5:2004 [15]. The two most common classes of soil, Classes C (shallow soil) and D (deep soil), were modelled. In this study, representative ground motions were selected for three geographical zones which covers:

1. North Island 1 (NI1) (Zone North A in Oyarzo-Vera et al. [16]) which includes Auckland, Hamilton & New Plymouth
2. North Island 2 (NI2) (Zone North NF in Oyarzo-Vera et al. [16]) which includes Wellington & Palmerston North
3. South Island 1 (SI1) (Tarbali and Bradley [17]) which covers Christchurch

For the North Island, Oyarzo-Vera et al. [16] considered deaggregations of a probabilistic seismic hazard model and the seismological characteristics of expected ground motions at different locations of the North Island (Figure 2). For this study, acceleration-time histories from two zones (Zone North A and Zone North NF) were used (Table 1 and Table 2). For Christchurch, ground motions recommended by Tarbali and Bradley [17], using the Generalized Conditional Intensity Measure approach, were used. Tarbali and Bradley [17] recommended ensembles of seven ground motions for each of the Alpine, Hope and Porters Pass earthquakes. For this study, a total of six ground motions (two motions from each earthquake) were selected for SI1 (Table 3).

Deconvolution of Acceleration-Time Records

As the OpenSees model requires velocity-time histories to be input at the base of the model, ground acceleration-time histories were first deconvolved (e.g., Meija & Dawson [18]) using STRATA [19] based on one-dimensional (1D) equivalent linear analyses. The deconvolved acceleration signals at the base of the 1D column were subsequently integrated to provide velocity-time histories that were applied at the base of the OpenSees model. In order to determine the reasonableness of acceleration-time histories at ground level which were propagated up from the base of the two-dimension OpenSees model, sample comparisons of the ground acceleration-spectra, frequency content (using Fast Fourier Transform analyses) and acceleration-time histories were carried out between the original acceleration-time histories and free-field acceleration-time histories from the OpenSees model. Variations of up to 20% in acceleration-spectra amplitudes were found in the comparisons and these were considered reasonable given the significant differences used in modelling (deconvolution based on equivalent linear analyses and the subsequent propagation of deconvolved signals based on non-linear assumptions made in OpenSees). For each of the deconvolved acceleration-time histories, approximately seven amplitude scalings were carried out to provide a range of $PGAs_{ff}$.

OPENSEES

Two-dimensional finite element (FE) analyses were performed for this project using OpenSees, which is an object-oriented open source software framework developed by the Pacific Earthquake Engineering Research Center (PEER). OpenSees allows users to simulate the responses of structural and geotechnical systems subjected to earthquakes [20]. It contains a large library of both linear and non-linear geotechnical and structural material models to enable realistic simulations. The software GiD [21] was used as a pre-processor to develop Tool Command Language (Tcl) scripts for OpenSees to create model meshes and, soil and structural nodes & elements. Outputs obtained from OpenSees were post-processed using Matlab [22].

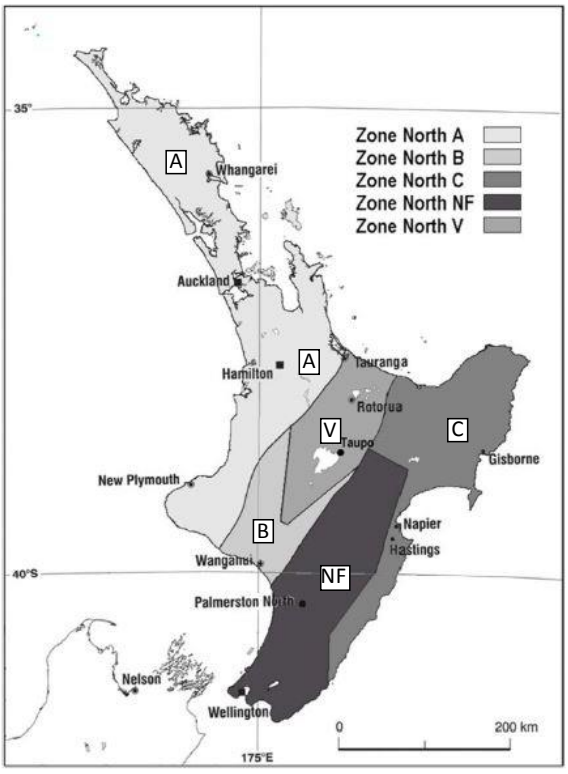

Figure 2: Geographical Zonation for North Island [16].

Table 1: Representative Ground Motions for North Island 1 – Zone A.

Soil Class	Event	Year	Mw*	Mechanism	PGA (g)
Class C	El Centro, Imperial Valley, USA	1940	7.0	Strike-Slip	0.21
	Delta, Imperial Valley, USA	1979	6.5	Strike-Slip	0.34
	Bovino, Campano Lucano, Italy	1980	6.9	Normal	0.05
	Kalamata, Greece	1986	6.2	Normal	0.23
	Matahina Dam D, Edgecumbe, NZ	1999	6.2	Strike-slip	0.28
Class D	El Centro, Imperial Valley, USA	1940	7.0	Strike-Slip	0.21
	Delta, Imperial Valley, USA	1979	6.5	Strike-Slip	0.34
	Kalamata, Greece	1986	6.2	Normal	0.23
	Corinthos, Greece	1981	6.6	Normal	0.31
	Westmorland, Superstition Hill, USA	1987	6.5	Strike-Slip	0.21

**Moment magnitude.*

Table 2: Representative Ground Motions for North Island 2 - Zone NF.

Soil Class	Event	Year	Mw*	Mechanism	PGA (g)
Class C	Duzce, Turkey	1999	7.1	Oblique	0.50
	Arcelik, Kocaeli, Turkey	1999	7.5	Strike-Slip	0.21
	La Union, Mexico	1985	8.1	Subduction interface	0.16
	Lucerne, Landers, USA	1992	7.3	Strike-Slip	0.60
	Tabas, Iran	1978	7.4	Reverse	0.93
Class D	El Centro, Imperial Valley, USA	1940	7.0	Strike-Slip	0.21
	Duzce, Turkey	1999	7.1	Oblique	0.50
	El Centro #6, Imperial Valley, USA	1979	6.5	Reverse	0.44
	Caleta de Campos, Mexico	1985	8.1	Subduction interface	0.14
	Yarimka YPT, Kocaeli, Turkey	1999	7.5	Strike-Slip	0.22

**Moment magnitude.*

Table 3: Representative Ground Motions for South Island 1 - Christchurch.

Soil Class	Record Sequence Number	Event	Year	Station	Mw*	Mechanism	PGA (g)
Classes C&D	Alpine fault scenario rupture						
	888	Landers	1992	San Bernardino - E & Hospitality	7.28	Strike-Slip	0.08
	1188	Chi-Chi, Taiwan	1999	CHY016	7.62	Reverse-Oblique	0.10
	Hope fault scenario						
	1147	Kocaeli, Turkey	1999	Ambarli	7.51	Strike-Slip	0.21
	1766	Hector Mine	1999	Baker Fire Station	7.13	Strike-Slip	0.11
	Porters Pass fault scenario						
	93	San Fernando	1971	Whittier Narrows Dam	6.61	Reverse	0.12
	1026	Northridge-01	1994	Lawndale - Osage Ave	6.69	Reverse	0.12

**Moment magnitude.*

Table 4: OpenSees Models.

Soil Class	Soil Profile/ Properties/Period	Wall Type
Class C – Shallow soils	Retained Fill comprising Medium dense Gravel (MDG) overlying 10m Medium dense Sand (MDS) overlying Bedrock. • MDG/MDS: ρ = 2000kg/m^3; ϕ'_{peak} = 36.5° • Calculated site period 0.28 secs.	1. Embedded cantilever wall; 2m retained soil height; 5m overall wall height. 2. Embedded cantilever; 3m retained soil height; 8m overall wall height. 3. Two-level propped wall; 3m retained soil height; 8m overall wall height. Props located at top of wall and 2.5m from top of wall have equal stiffness.
Class D – Deep soils	Retained Fill comprising Medium dense Gravel (MDG) overlying 6m Medium dense Sand (MDS) overlying 10m Loose Sand (LS) overlying Bedrock. • MDG/MDS: ρ = 2000kg/m^3; ϕ'_{peak} = 36.5° • LS: ρ = 1800kg/m^3; ϕ'_{peak} = 32° • Calculated site period of 0.84 secs.	4. Embedded cantilever; 2m retained soil height; 5m overall wall height. 5. Embedded cantilever; 3m retained soil height; 8m overall wall height. 6. Two-level propped wall; 3m retained soil height; 8m overall wall height. Props located at top of wall and 2.5m from top of wall have equal stiffness.

Two-Dimensional Models

Six two-dimensional base models were created within OpenSees to model variations in soil class, wall types and retained soil heights (Table 4). All wall properties were based on 750mm diameter reinforced concrete piles at 2.25m spacing. Free-field site periods based on the retained soil profile were calculated using the method by Dobry and Madera (described by Larkin and Van Houtte [23]).

Back-filling behind the retaining wall with Fill comprising medium dense gravel was modelled by placing fill in 1m lifts. Examples of a Class C propped wall and a Class D embedded cantilever wall (3m retained height) are given in Figure 3 and Figure 4 respectively. The selection of soil element size in the OpenSees model was based on the recommendation of Kuhlemeyer and Lysmer [24] and Smith [25] that the element length in the direction of propagation should be less than one-eighth of the shortest wave length. An initial approximation of an appropriate maximum element length was based on a

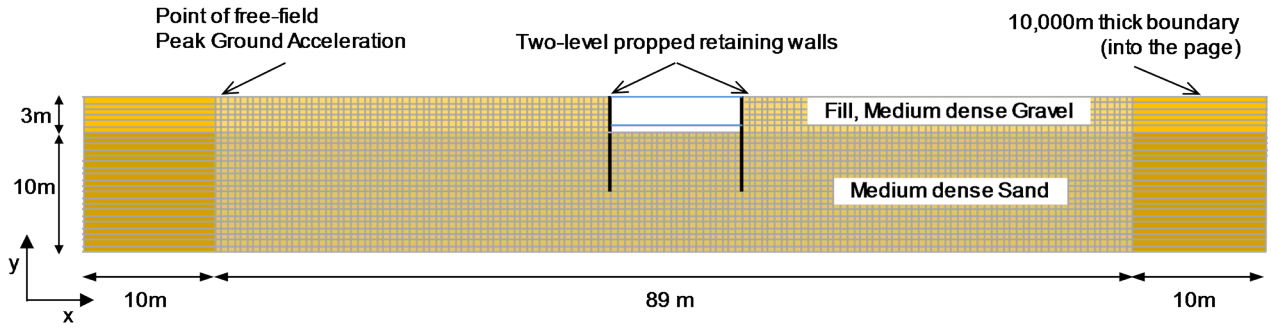

Figure 3: Example of Class C propped wall in OpenSees.

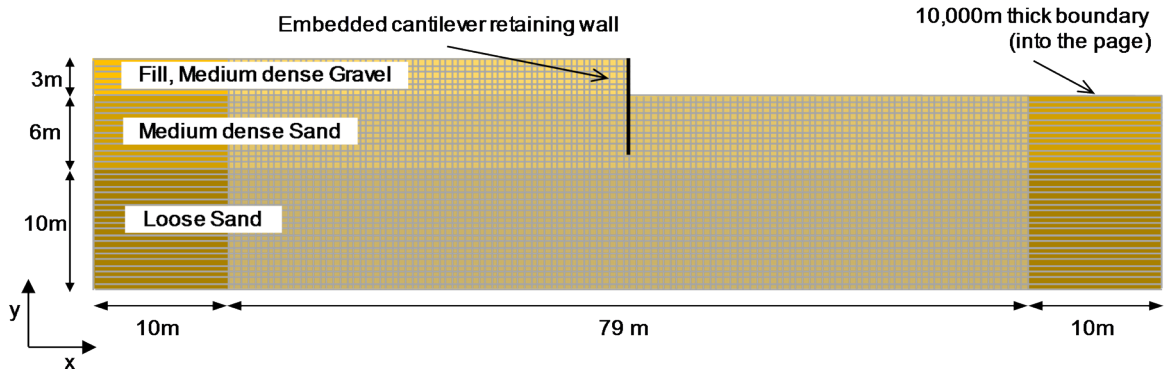

Figure 4: Example of Class D embedded cantilever wall in OpenSees.

maximum shear wave frequency of 15Hz (e.g., Zhang et al. [26]) and an average shear wave velocity of ~140m/s. This suggested a maximum element length of 1m. The final soil element mesh adopted for all analyses was a 0.5m x 0.5m mesh with an element thickness of 1.0m (into the page). In order to maintain free-field conditions at the left and right boundaries at the ground surface, two free-field columns with increased widths (10m wide each) and significant thickness (10,000m into the page) were assigned to the model. With the base of these massive free-field columns connected using Equal Degree of Freedom (EqualDOF) connections at the base nodes, horizontal excitation applied to the base of these columns would result in a free-field response of the columns (after McGann and Arduino [27]). Subsequent assessments of mean periods for all runs as defined by Rathje et al. [28] confirmed the appropriateness of an element length of 0.5m in accordance to Kuhlemeyer and Lysmer [24] and Smith [25]. Rayleigh damping to all elements and nodes was set to a damping ratio of 5%, which provided a reasonable match of free-field spectra and acceleration magnitude results between one-dimensional equivalent linear analysis (using STRATA) and two-dimensional OpenSees models.

Materials

Soil properties were modelled using the PressureDependMultiYield02 (PDMY02) material from OpenSees, which is an elastic-plastic material specially created to simulate a non-linear stress-strain relationship under general loading conditions. Characteristics of PDMY02 include dilatancy (shear-induced volume contraction or dilation) and non-flow liquefaction (cyclic mobility), typically exhibited in sands or silts during monotonic or cyclic loading. Under gravity (static) loading, the material behaviour is linear elastic. In subsequent dynamic loading phases, the stress-strain response is elastic-plastic. Plasticity is formulated based on the multi-surface (nested surfaces, see Figure 5) concept, with a non-associative flow rule to reproduce the dilatancy effect. All soils were modelled as dry. Shear modulus variations with mean effective confining stresses were derived by the PDMY02 material. Some examples of these relations are shown in Figure 6a and b.

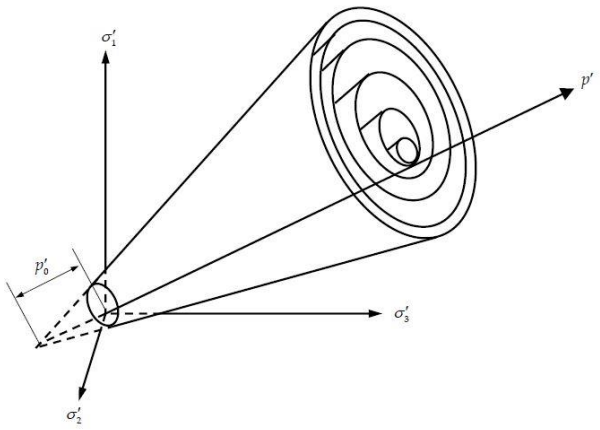

Figure 5: Conical nested yield surfaces in principal stress space (after Parra-Colmenares [29])

Elements

Soil elements were modelled with SSPQuad elements which are four noded quadrilateral elements using stabilised single point integration with a single Gauss integration point in the centre of each element, with two degrees of freedom (2DOF). The retaining wall was modelled using ElasticBeamColumn elements with three degrees of freedom (3DOF). Where a propped wall was modelled, two levels of props were used. The pair of props was modelled as massless, elastic members

with the same stiffness properties. Sensitivity runs were carried out with two pairs of props, each pair with different stiffnesses.

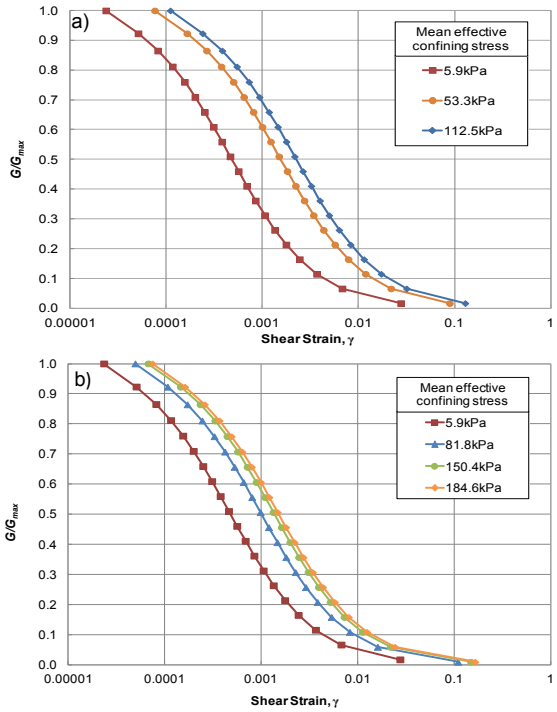

Figure 6: Examples of derived G/G_{max} curves for PDMY02 model for a) Class C soil model and b) Class D soil model at various mean effective confining stresses.

Connections between soil and wall were established with ZeroLength Elements (ZLE) and EqualDOFs. The ZLEs represent the interface between soil and wall and the EqualDOFs allows the connection between 2DOF (soil) and 3DOF (wall) elements. Two materials were chosen to model the soil-wall interface. In the x-direction, a uniaxial Elastic-No Tension (ENT) material was chosen and in y-direction an Elastic-Perfectly Plastic (ElasticPP) material. The uniaxial ENT material allows soil to act in compression against the wall and to allow separation to occur when soil moves away from the wall. The uniaxial ENT material varied with depth (0.5m intervals according to the mesh) and was based on the Young's Modulus of the surrounding soil. The ElasticPP material was similarly modelled at 0.5m intervals with an assumed stiffness of 3900 kPa (based on Drumm & Desai [30]) at every 0.5m depth. Varying limiting strains were defined to model plastic behaviour based on a maximum allowable ratio of soil-wall friction (δ/φ') of 0.5.

Boundary Conditions

As discussed above, free-field boundary conditions were modelled using 10m wide and 10,000m thick (into the page) columns (Figure 3 and Figure 4). In static conditions the base was fixed in x- and y-directions. For dynamic analysis, the boundary conditions at the base were changed to allow fixity in the y-direction only, as shown in Figure 7. The earthquake motion was applied as a velocity-time history (by integrating the respective deconvolved acceleration-time history) in the x-direction to node number 1, which was the overall master node. Node 1 was connected with equal DOF (in x-direction only) to all base nodes (1 to 2, 1 to 3, 1 to 4, etc.) as well as to the dashpot node. This ensured that the earthquake motion would be applied along the entire base of the model. Within each free-field boundary column, nodes were connected horizontally via EqualDOFs as shown in Figure 7 below.

Analyses

The in-situ static stress state of the model was achieved by building up the model in 1m soil lifts. At the end of the static state and prior to carrying out a dynamic analysis, in-situ soil stresses were checked and both bending moments & shear forces in the wall were compared with results from WALLAP version 6.05 [31]. The Krylov Newton algorithm was selected, which was found to be generally faster than other Newtonian algorithms and more stable compared to other methods [32]. The dynamic active force (ΔP_{AE}) defined as the incremental force exceeding the static force, acting over the retained soil height on the active side of the retaining wall during a seismic event was determined using OpenSees and the three pseudo-static methods (Rigid, Stiff and Flexible wall solutions) described earlier.

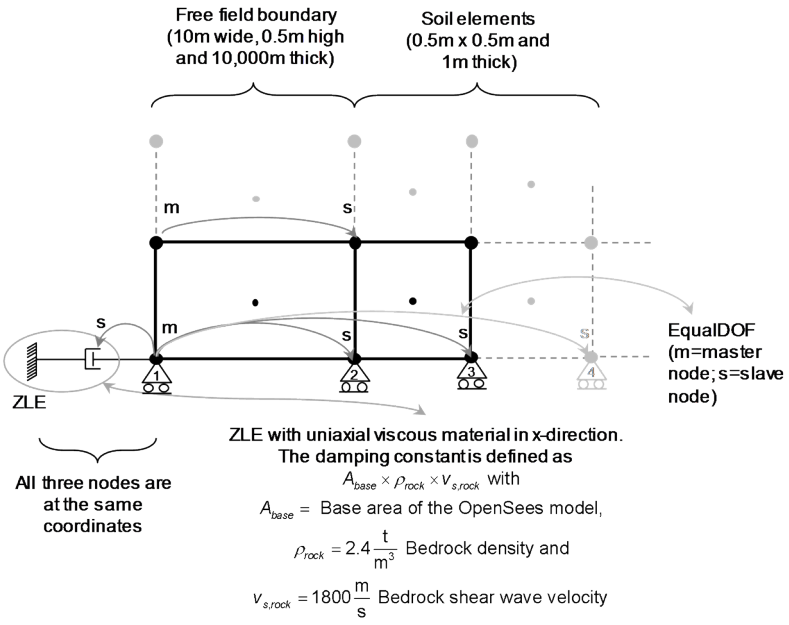

Figure 7: Boundary conditions at base of model during dynamic analysis.

The intention was to compare the maximum ΔP_{AE} obtained from OpenSees with the other three pseudo-static methods based on PGA_{ff} obtained from each OpenSees run (PGA_{ff} based on free-field conditions at the level of the top of retaining wall, see Figure 3). These comparisons were assessed against wall displacements predicted in OpenSees. Where ΔP_{AE} was calculated using results from OpenSees, this was denoted by the term $\Delta P_{AE,OpenSees}$. Forces in the Elastic No-Tension Zero-Length elements (ENT-ZLEs) which connect the soil to the wall were integrated over the retained soil height for each time step of the dynamic analysis. $\Delta P_{AE,OpenSees}$ was determined at each time step by subtracting the integrated force measured in the ENT-ZLEs at the end of static loading from those recorded during the seismic shaking. For a given dynamic run, the maximum $\Delta P_{AE,OpenSees}$ was used to compare against ΔP_{AE} calculated using other pseudo-static methods as described in Equation (1), (2) and (3) below.

- Calculate ΔP_{AE} using the Rigid wall solution [4, 5]:

$$\Delta P_{AE,Rigid\ Wall,X\%PGA} = C(0).\gamma.H^2 \quad (1)$$

- Calculate ΔP_{AE} using the Stiff wall solution [4, 5]:

$$\Delta P_{AE,Stiff\ Wall,X\%PGA} = 0.75\ C(0).\gamma.H^2 \quad (2)$$

- Calculate ΔP_{AE} using the Flexible wall solution (Mononobe-Okabe (M-O) method):

$$\Delta P_{AE,M-O,X\%PGA} = \frac{1}{2}(K_{AE} - K_A).\gamma.H^2 \quad (3)$$

The seismic coefficient, $C(0)$, is referred to as a fraction of PGA_{ff}/g based on the percentage of PGA_{ff} denoted by the subscript $_{X\%PGA}$, where X is the percentage of PGA_{ff}. For example, $\Delta P_{AE,Stiff\ Wall,80\%PGA}$ indicates that 80% of PGA_{ff} expressed as a fraction of g was assumed to be the seismic coefficient. The wall friction coefficient in the M-O calculation was assumed to be 0.5 to coincide with assumptions made in OpenSees. In addition, the average wall displacement (Δh_{avg}) due to both static and dynamic loads over the retained height of the retaining wall in the OpenSees analyses as follows:

$$\Delta h_{avg} = \frac{\sum_{i=1}^{n}(\Delta h_{t,max,i} - \Delta h_{ff,t,max,i})}{n} \quad (4)$$

Where n is the number of wall nodes over the exposed wall height, $\Delta h_{t,max}$ is the maximum absolute displacement profile of the wall at a given time, t during the seismic event and $\Delta h_{ff,t,max}$ is the free-field soil displacement profile at the time of $\Delta h_{t,max}$. It was noted that the displacement profile at time of $\Delta h_{t,max}$ may not coincide with the time of maximum $\Delta P_{AE,OpenSees}$.

RESULTS

For each of the wall base models described in Table 4, scaled velocity-time histories related to the North and South Island were applied to the model. A total of 946 OpenSees runs were carried out and for each run, the PGA_{ff} was established. These PGA_{ff}'s were used to calculate $\Delta P_{AE,Rigid\ Wall}$, $\Delta P_{AE,Stiff\ Wall}$ and $\Delta P_{AE,M-O}$ and comparisons were made against $\Delta P_{AE,OpenSees}$. A moderately conservative approach was used to determine an appropriate fraction of PGA_{ff} to use in the pseudo-static analyses so that forces estimated using the pseudo-static analyses would either match or over-estimate dynamic active forces calculated using OpenSees. Results of these correlations for shallow soils (Class C) are found in Figure 8, Figure 9 and Figure 10 for NI1, NI2 and SI1 respectively and for deep soils (Class D) results are found in Figure 11, Figure 12 and Figure 13. Results of all 946 individual runs are reported by Chin and Kayser [33].

It is clear from interpreting the OpenSees results, as summarised in Figures 8 to 13, that the dynamic active force (ΔP_{AE}) is a function of wall displacements. An opportunity was taken to revise the displacement criteria from "top of wall" (as suggested by Matthewson et al. [4] and Wood & Elms [5]) to an average wall displacement over the height of the retained soil. This was undertaken to address the issue that maximum displacements do not necessarily always occur at the top of wall and also to acknowledge that the overall displaced profile of the wall, rather than the displacement at the top of the wall greatly affects the resultant dynamic active force. The results demonstrate that seismic earth forces are sensitive to and dependent on wall displacements, geographical zones (reflecting unique seismic signatures) and soil classes. The usefulness of simple pseudo-static analyses in approximating moderately conservative maximum dynamic earth forces based on optimised PGA_{ff}'s, wall displacements, geographical zones and soil classes is demonstrated. A summary of the results showing percentages of PGA_{ff} used in simplified pseudo-static methods for given ranges of normalised average wall displacements are given in Table 5.

The results indicate that for a given geographic location and wall displacement range, the modelled soil Class D site generates larger dynamic earth pressures against the wall compared with Class C soil class. The reason for this will require additional investigation. Further results from OpenSees indicate that resultant locations of the total dynamic active force, P_{AE} (comprising both static and dynamic forces) typically act at $0.7H$ from the top of the wall (where H is the retained soil height). This agrees approximately with the 2/3rd H recommendation of Wood & Elms [5] and also with Atik & Sitar [14, 34]. An assessment of the times at which the maximum PGA_{ff} occurred compared to when the maximum dynamic active force occurred showed that in ~80% of all the runs, the occurrences of maximum PGA_{ff} and $\Delta P_{AE,OpenSees}$ did not coincide. In the majority of the cases, maximum $\Delta P_{AE,OpenSees}$ occurred after the occurrence of maximum PGA_{ff}. An assessment of the times at which the maximum PGA_{ff} occurred compared to when the maximum wall bending moment occurred showed that in ~72% of all the runs, the occurrences of maximum PGA_{ff} did not coincide with the time of maximum bending moment. Additionally, in ~68% of all the runs, the occurrence of maximum dynamic active force, ΔP_{AE}, did not coincide with the times at which maximum wall bending moment occurred. A similar finding was reported in centrifuge test results by Atik & Sitar [14], who attributed this to out of phase soil and wall displacements. Although it could be considered conservative to assume the concurrence of maximum dynamic active force with maximum bending moment, this assumption is recommended on the basis that in some 32% of the runs, this occurrence took place.

SUMMARY AND CONCLUSION

This study has used a two-dimensional non-linear dynamic finite element program, OpenSees to determine seismic soil thrusts acting on retaining walls. The three main objectives of this study were to investigate the following:

1. Compare seismic soil thrusts from OpenSees modelling against pseudo-static analytical methods such as the Rigid, Stiff and Flexible wall solutions & determine if a reduction (or increase) to free-field PGA, applied as a seismic coefficient to these solutions, can be justified.
2. Identify the range of wall displacements applicable to the pseudo-static solutions.

3. Determine the location of seismic active soil thrust acting on the retaining wall.

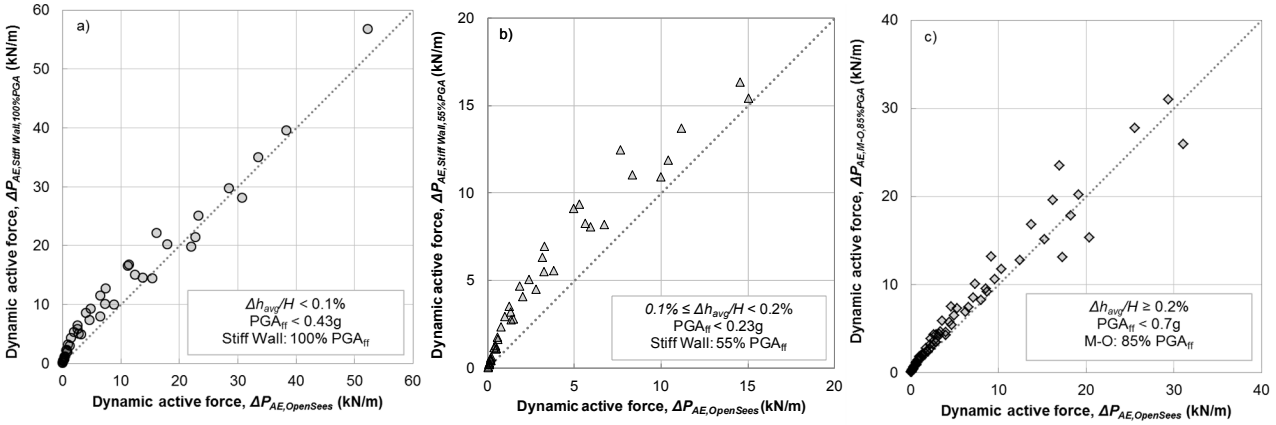

Figure 8: North Island 1 Soil Class C, comparison of Dynamic active forces from OpenSees vs. Pseudo-Static solutions for a) ($\Delta h_{avg}/H$) < 0.1%, Stiff wall 100% PGA_{ff}, b) 0.1% ≤ ($\Delta h_{avg}/H$) < 0.2%, Stiff wall 55% PGA_{ff} and c) ($\Delta h_{avg}/H$) ≥ 0.2%, Flexible wall 85% PGA_{ff}.

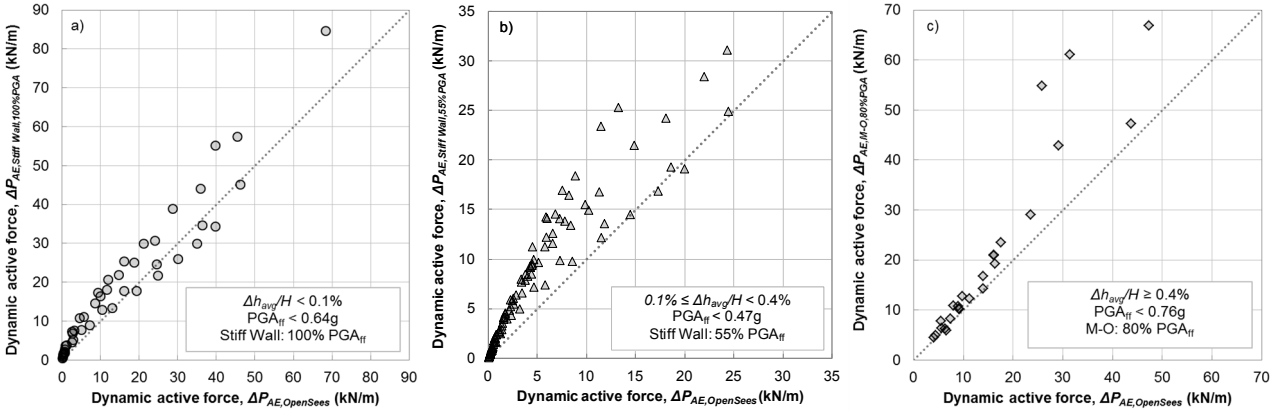

Figure 9: North Island 2 Soil Class C, comparison of Dynamic active forces from OpenSees vs. Pseudo-Static solutions for a) ($\Delta h_{avg}/H$) < 0.1%, Stiff wall 100% PGA_{ff}, b) 0.1% ≤ ($\Delta h_{avg}/H$) < 0.4%, Stiff wall 55% PGA_{ff} and c) ($\Delta h_{avg}/H$) ≥ 0.4%, Flexible wall 80% PGA_{ff}.

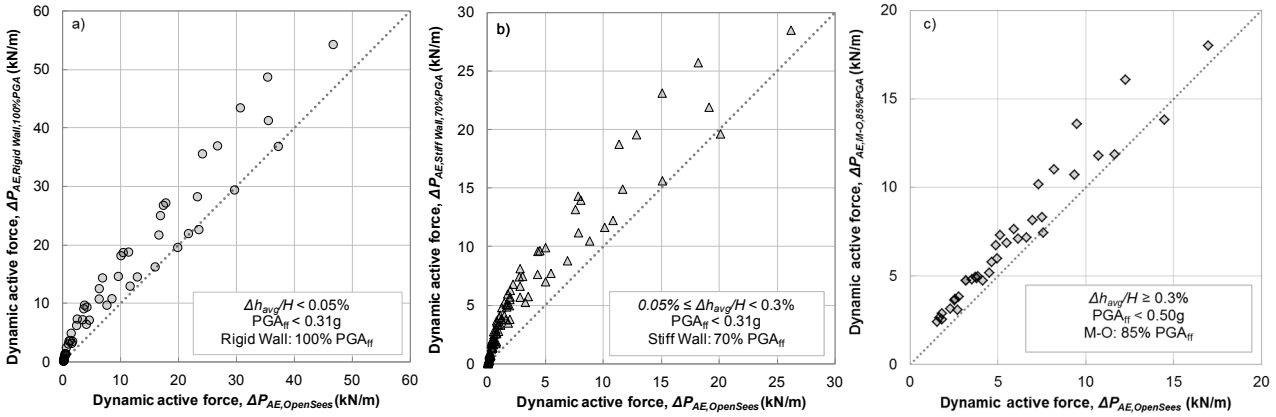

Figure 10: South Island 1 Soil Class C, comparison of Dynamic active forces from OpenSees vs. Pseudo-Static solutions for a) ($\Delta h_{avg}/H$) < 0.05%, Rigid wall 100% PGA_{ff}, b) 0.05% ≤ ($\Delta h_{avg}/H$) < 0.3%, Stiff wall 70% PGA_{ff} and c) ($\Delta h_{avg}/H$) ≥ 0.3%, Flexible wall 85% PGA_{ff}.

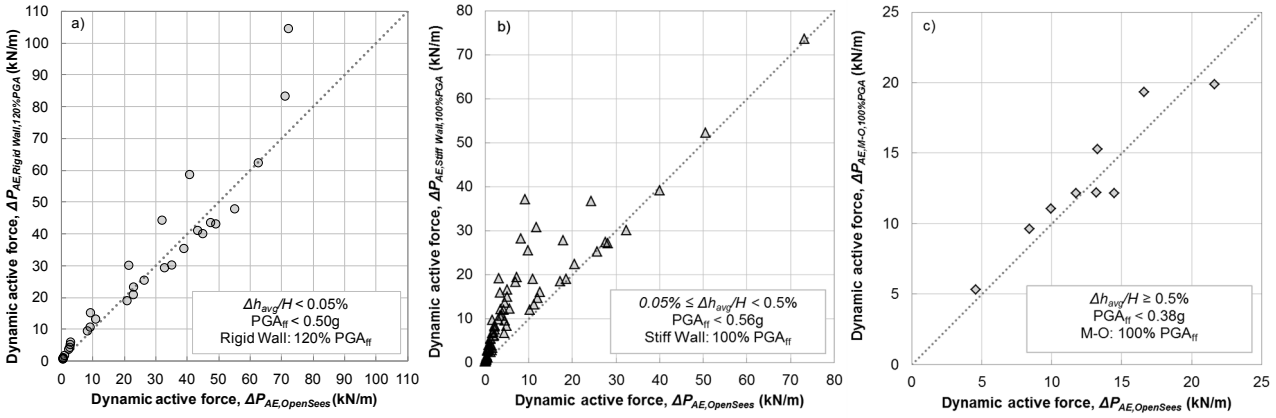

Figure 11: North Island 1 Soil Class D, comparison of Dynamic active forces from OpenSees vs. Pseudo-Static solutions for a) $(\Delta h_{avg}/H) < 0.05\%$, Rigid wall 120% PGA_{ff}, b) $0.05\% \le (\Delta h_{avg}/H) < 0.5\%$, Stiff wall 100% PGA_{ff} and c) $(\Delta h_{avg}/H) \ge 0.5\%$, Flexible wall 100% PGA_{ff}.

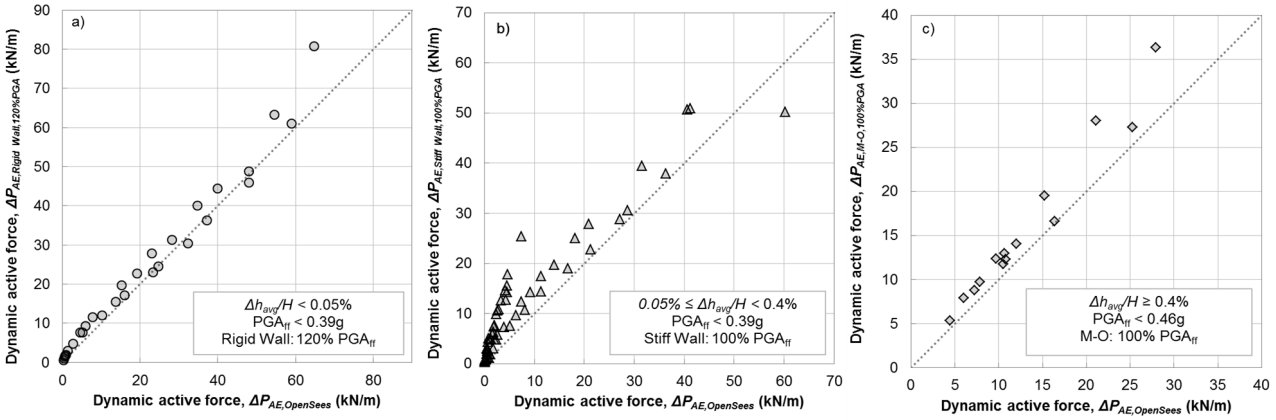

Figure 12: North Island 2 Soil Class D, comparison of Dynamic active forces from OpenSees vs. Pseudo-Static solutions for a) $(\Delta h_{avg}/H) < 0.05\%$, Rigid wall 120% PGA_{ff}, b) $0.05\% \le (\Delta h_{avg}/H) < 0.4\%$, Stiff wall 100% PGA_{ff} and c) $(\Delta h_{avg}/H) \ge 0.4\%$, Flexible wall 100% PGA_{ff}.

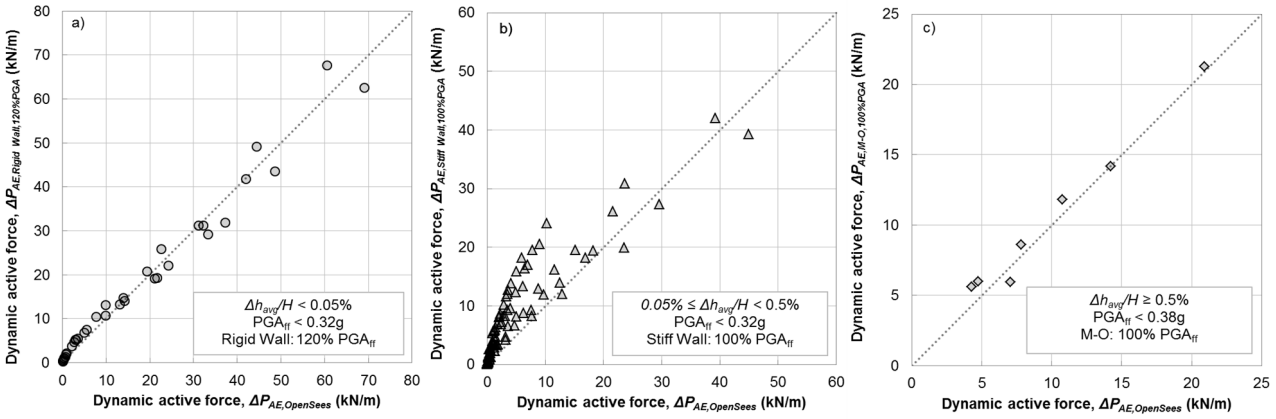

Figure 13: South Island 1 Soil Class D, comparison of Dynamic active forces from OpenSees vs. Pseudo-Static solutions for a) $(\Delta h_{avg}/H) < 0.05\%$, Rigid wall 120% PGA_{ff}, b) $0.05\% \le (\Delta h_{avg}/H) < 0.5\%$, Stiff wall 100% PGA_{ff} and c) $(\Delta h_{avg}/H) \ge 0.5\%$, Flexible wall 100% PGA_{ff}.

The above study was limited to three geographical zones in New Zealand. These are described in the report as:

- North Island 1 which includes Auckland, Hamilton & New Plymouth,
- North Island 2 which includes Wellington & Palmerston North
- South Island 1 which covers Christchurch.

OpenSees was used to model embedded cantilever and propped retaining walls in two different soil classes. These soil classes were Class C (shallow soils) and Class D (deep soils) in accordance with New Zealand Standard 1170.5 [15]. As is commonly used in the study of seismic actions on structures (e.g., NZS 1170.5:2004 [15] clause 5.5), a suite of appropriate

acceleration-time histories appropriate for the above three geographical zones and soil class were established for this study. These motions were deconvolved from the ground surface to the base of the model using one-dimensional equivalent linear analysis (STRATA [19]) and subsequently integrated to provide velocity-time history records applied to the base of the OpenSees model. Additional scaling of the deconvolved acceleration amplitudes were carried out to model varying amplitudes of motions. A total of 946 runs were conducted in OpenSees. To account for non-linearity in the soil's response to seismic loading, a variation of the Pressure Dependent Multi-Yield constitutive material (PDMY02) was used to model soil in OpenSees. This allowed for elastic-plastic behaviour simulating a non-linear stress-strain relationship. The model was based on dry soil with no liquefaction.

Results of seismic soil thrusts from OpenSees analyses and the three pseudo-static methods showed some interesting correlations. These demonstrated that by selecting the correct fraction of free-field PGA based on the geographical zone, pseudo-static methods can be used to determine moderately conservative estimates of the maximum seismic soil thrust subject to the appropriate wall displacement response. Hence, the current industry-standard method of carrying out a series of iterative calculations which match the assumed wall displacement associated with a particular pseudo-static method with the derived wall displacement remains a reasonable way to carry out this analysis. A range of fractions of free-field PGAs applied as Peak Ground Acceleration Coefficients in pseudo-static methods was obtained; from as low as 55% of PGA_{ff} in a stiff wall solution (e.g., for North Island 1, Class C, $0.1\% \leq (\Delta h_{avg}/H) < 0.2\%$) to 120% of PGA_{ff} in a rigid wall solution (e.g., for North Island 1, Class D, $(\Delta h_{avg}/H) < 0.05\%$). This study has established the sensitivity of the maximum seismic soil thrust to normalised average wall displacements. For each of the geographical zones and soil classes studied, the maximum seismic soil thrust could be attributed to different ranges of wall displacements. It was noted that these ranges were different for different geographic locations or soil class. The total dynamic active force was found to act typically at $0.7H$ (where H is the retained soil height) from the top of the wall. It is recommended that until further evidence becomes available, a reasonably conservative design approach would be to include inertial loading of the wall acting concurrently with the maximum dynamic active force. It is important to note that the results presented in this study should be considered to be applicable only within the parameters considered. It is clear, for example, that changes in soil properties behind the retaining wall could generate different results. Additional analyses to include acceleration time-histories appropriate to the remainder of the North and South Island would be useful. In addition, research incorporating other variations in parameters such as wall heights, wall types, walls sited on slopes and other soil combinations within a given soil class would be very beneficial.

Table 5: Seismic coefficients for use in pseudo-static analysis.

Geographical location	Soil class	Normalised average wall displacements due to static & dynamic loads ($\Delta h_{avg}/H$)%	Seismic coefficient (%PGA_{ff}) used in pseudo-static calculations		
			Flexible (M-O)	Stiff	Rigid
North Island 1	C	< 0.1	-	100	-
		≥ 0.1 and < 0.2	-	55	-
		≥ 0.2	85	-	-
	D	< 0.05	-	-	120
		≥ 0.05 and < 0.5	-	100	
		≥ 0.5	100	-	-
North Island 2	C	< 0.1	-	100	-
		≥ 0.1 and < 0.4	-	55	-
		≥ 0.4	80	-	-
	D	< 0.05	-	-	120
		≥ 0.05 and < 0.4	-	100	-
		≥ 0.4	100	-	-
South Island 1	C	< 0.05	-	-	100
		≥ 0.05 and < 0.3	-	70	-
		≥ 0.3	85	-	-
	D	< 0.05	-	-	120
		≥ 0.05 and < 0.5	-	100	-
		≥ 0.5	100	-	-

ACKNOWLEDGMENTS

The first two authors gratefully acknowledge the financial support of the Earthquake Commission and the University of Canterbury Quake Centre in the award of Industry fellowships. The generosity of the University of Auckland in hosting the first two authors for the period of research is acknowledged.

REFERENCES

1 NZ Transport Agency (2014). "Bridge Manual (SP/M/022)", 3rd Edition, Amendment 1, 310 pp.

2 Okabe, S (1926). "General Theory of Earth Pressures". *Journal of Japan Society of Civil Engineers*, **12**(1): 123-134.

3 Mononobe, N and Matsuo, M (1929). "On the Determination of Earth Pressures during Earthquakes". *Proceedings: World Engineering Congress*, Japan, Tokyo, October – November 1929, **9**, Paper No. 388,179-187.

4 Matthewson, MB, Wood, JH and Berrill, JB (1980). "Seismic Design of Bridges" Section 9: Earth Retaining Structures. *Bulletin of the New Zealand National Society for Earthquake Engineering*, **13**(3): 280-293.

5 Wood, JH and Elms, DG (1990). *"Seismic Design of Bridge Abutments and Retaining Walls"*. Transit New Zealand, Road Research Unit, **84**(2).

6 Wood, JH (1973). *"Earthquake-Induced Soil Pressures on Structures"*. PhD Thesis, California Institute of Technology, Pasadena, California, 327 pp.

7 Seed, HB and Whitman, RV (1970). "Design of Earth Retaining Structures for Dynamic Loads". *Proceedings: ASCE Specialty Conference on Lateral Stresses in the Ground and Design of Earth-Retaining Structures*, United States, New York, Ithaca, June 1970, 103-147.

8 Greek Regulatory Guide E39/93 (1998). "*Regulatory Guide E39/93 for the Seismic Analysis of Bridges*". Bulletin of Greek Technical Chamber No. 2040, Ministry of Public Works, Athens (in Greek).

9 Green, RA, Olgun, CG, Ebeling, RM and Cameron, WI (2003). "Seismically Induced Lateral Earth Pressures on a Cantilever Retaining Wall". *Proceedings of the 6th U.S. Conference and Workshop on Lifeline Earthquake Engineering* (TCLEE), Advancing Mitigation Technologies and Disaster Response, USA, California, Long Beach, 10 – 13 August 2003, 946-955.

10 Steedman, RS and Zeng, X (1990). "The Influence of Phase on the Calculation of Pseudo-Static Earth Pressure on a Retaining Wall". *Geotechnique* **40**(1): 103-112.

11 Gazetas, G, Psarropoulos, PN, Anastasopoulos, I, and Gerolymos, N (2004). "Seismic Behaviour of Flexible Retaining Systems Subjected to Short-Duration Moderately Strong Excitation". *Soil Dynamic and Earthquake Engineering*, **24**(7): 537-550.

12 Psarropoulos, PN, Klonaris, G, and Gazetas, G (2005). "Seismic Earth Pressures on Rigid and Flexible Retaining Walls". *Journal of Soil Dynamics and Earthquake Engineering*, **25**(7-10), 795-809.

13 Anderson, DG, Martin, GR, Lam, I and Wang, JN (2008). "*Seismic Analysis and Design of Retaining Walls, Buried Structures, Slopes and Embankments*". National Cooperative Highway Research Program, Report 611, 148 pp.

14 Atik, LA and Sitar, N (2010). "Seismic Earth Pressures on Cantilever Retaining Structures". *Journal of Geotechnical and Geoenvironmental Engineering*, **136**(10): 1324-1333.

15 Standards New Zealand (2004). "NZS 1170.5: Structural Design Actions. Part 5: Earthquake Actions – New Zealand". Standards New Zealand, Wellington, 80 pp.

16 Oyarzo-Vera, C, McVerry, GH and Ingham, JM (2012). "Seismic Zonation and Default Suite of Ground-Motion Records for Time-History Analysis in the North Island of New Zealand". *Earthquake Spectra*, **28**(2): 667-688.

17 Tarbali, K and Bradley, BA (2014). "Representative Ground-Motion Ensembles for Several Major Earthquake Scenarios in New Zealand". *Bulletin of the New Zealand Society for Earthquake Engineering*, **47**(4): 231-252.

18 Mejia, LH and Dawson, EM (2006). "Earthquake Deconvolution for FLAC". *Proceedings of the 4th International FLAC Symposium on Numerical Modelling in Geomechanics*. Spain, Madrid, 29 – 31 May 2006, 211-219.

19 STRATA (2013). Rathje, EM and Kottke, A, https://nees.org/resources/strata (Accessed 06/10/2015).

20 OpenSees (2006). OpenSees. http://opensees.berkeley.edu/. (Accessed 06/10/2015).

21 GiD. http://www.gidhome.com. (Accessed 06/10/2015).

22 MATLAB. http://www.mathworks.com (Accessed 06/10/2015).

23 Larkin, T and Van Houtte, C (2014). "Determination of Site Period for NZS1170.5:2004). *Bulletin of the New Zealand Society for Earthquake Engineering*, 47(1): 28-40.

24 Kuhlemeyer, RL and Lysmer, J (1973). "Finite Element Accuracy for Wave Propagation Problems". *Journal of Soil Mechanics and Foundations Division*, Proc. ASCE, **99**(SM5): 421-427.

25 Smith, WD (1975). "The Application of Finite Element Analysis to Body Wave Propagation Problems". *Geophysical Journal of the Royal Astronomical Society*, **42**(2): 747-768.

26 Zhang, Y, Conte, JP, Yang, Z, Elgamal, A, Bielak, J and Acero, G (2008). "Two-Dimensional Nonlinear Earthquake Response Analysis of a Bridge-Foundation-Ground System". *Earthquake Spectra* **24**(2): 343-386.

27 McGann, CR and Arduino, P (2015). *"Dynamic 2D Effective Stress Analysis of Slope"*, http://opensees.berkeley.edu/wiki/index.php/Dynamic_2D_Effective_Stress_Analysis_of_Slope (Accessed 10/10/2015).

28 Rathje, EM, Faraj, F, Russell, S and Bray, J (2004). "Empirical Relationships for Frequency Content Parameters of Earthquake Ground Motions". *Earthquake Spectra*, **20**(1): 119-144.

29 Parra-Colmenares, EJ (1996). *"Numerical Modeling of Liquefaction and Lateral Ground Deformation Including Cyclic Mobility and Dilation Response in Soil Systems"*. PhD Thesis, Rensselaer Polytechnic Institute, Troy, NY.

30 Drumm, EC and Desai, CS (1986). "Determination of Parameters for a Model for the Cyclic Behaviour of Interfaces". *Earthquake Engineering and Structural Dynamics*, **14**: 1-18.

31 Geosolve (2013). WALLAP Retaining Wall Analysis Program. Version 6.05 Revision A45.B58.R49 April 2013

32 Scott, MH and Fenves, GL (2010). "Krylov Subspace Accelerated Newton Algorithm: Application to Dynamic Progressive Collapse Simulation of Frames". *Journal of Structural Engineering*, **136**(5): 473-480.

33 Chin, CY and Kayser, C (2016). "*Seismic Pressures on Retaining Walls*". University of Canterbury Quake Centre report, dated 14/03/16, 2913 pp.

34 Atik, LA and Sitar, N (2008). *"Experimental and Analytical Study of the Seismic Performance of Retaining Structures"*. Pacific Earthquake Engineering Research Center (PEER) Report 2008/104, Department of Civil and Environmental Engineering, University of California, Berkeley, 295 pp.